

Tritium transport model at breeder unit level for WCLL breeding blanket

*Original*

Tritium transport model at breeder unit level for WCLL breeding blanket / Candido, Luigi; Testoni, Raffaella; Utili, Marco; Zucchetti, Massimo. - In: FUSION ENGINEERING AND DESIGN. - ISSN 0920-3796. - STAMPA. - (2019).  
[10.1016/j.fusengdes.2019.02.041]

*Availability:*

This version is available at: 11583/2729090 since: 2019-03-21T10:58:07Z

*Publisher:*

Elsevier Ltd

*Published*

DOI:10.1016/j.fusengdes.2019.02.041

*Terms of use:*

This article is made available under terms and conditions as specified in the corresponding bibliographic description in the repository

*Publisher copyright*

(Article begins on next page)

# Tritium Transport Model at Breeder Unit Level for WCLL Breeding Blanket

Luigi Candido<sup>a</sup>, Raffaella Testoni<sup>a</sup>, Marco Utili<sup>b</sup>, Massimo Zucchetti<sup>a</sup>

<sup>a</sup> Dipartimento Energia, Politecnico di Torino, Corso Duca degli Abruzzi 24 – Torino, Italy

<sup>b</sup> ENEA UTIS- C.R. Brasimone, Bacino del Brasimone, Camugnano, BO, Italy

In a fusion power demonstration plant (DEMO), the development of a tritium transport model is mandatory in order to correctly predict the tritium concentration inside the liquid metal, the permeated flux through the structural materials and into the coolant, playing a fundamental role in guaranteeing tritium self-sufficiency in the fusion reactor and safety both for the workers and for the external environment. In the present work, a multi-physics 3D tritium transport model has been assessed for a single breeder unit located in the outboard equatorial module of the Water-Cooled Lithium Lead (WCLL) breeding blanket of DEMO, adopting an approach that permits to have a modelling tool able to be adaptive within certain margins to changes in operating parameters and geometry. The transport has been modelled considering advection-diffusion of tritium into the lead-lithium eutectic alloy, transfer of tritium from the liquid interface towards the steel (adsorption/desorption), diffusion of tritium inside the steel, transfer of tritium from the steel towards the coolant (recombination/dissociation), advection-diffusion of diatomic tritium into the coolant. The effect of buoyancy forces, which arise due to temperature variation, has been also considered. Under the above-specified phenomena, tritium concentrations, inventories and losses have been derived.

Keywords: breeding blanket, DEMO, WCLL, tritium transport, buoyancy effect

## 1. Introduction

In the frame of the EUROfusion Consortium, which aims to develop a conceptual design of the fusion power demonstration plant (DEMO) within the “Horizon 2020” roadmap [1, 2], various integrated power plants and physics technologies projects are being conducted, including the Breeder Blanket (BB) project. The Water-Cooled Lithium Lead (WCLL) breeding blanket is one of the four European blanket concepts proposed for the DEMO reactor [3] to meet this goal.

The study of tritium transport inside the blanket is fundamental to assess its preliminary design and safety features. One of the main neutronic requirements for DEMO, needed to fulfil a reliable operation, is to ensure tritium self-sufficiency [4]. Moreover, from the point of view of safety, the amount of tritium permeated towards the coolant and towards the environment must be kept under a certain level [5] in order to reduce the risk of potential radiological hazard.

This paper presents a tritium transport study at the minimal functional unit (breeder unit) level in the outboard equatorial module of WCLL, which is one of the most thermally loaded modules in normal operating conditions. The breeder unit approach permits to have a modelling tool that can be easily adapted – within certain margins – to changes in operating parameters and geometry. The calculations have been performed by means of COMSOL Multiphysics 5.3a [6]. In this paper, the results concerning tritium concentrations, inventories and losses will be shown. In particular, the influence of buoyancy effect on tritium transport has been investigated.

## 2. Description of the model

The geometry of the reference breeder unit is referred to the DDD 2015 baseline [7] (see Fig.1). The module consists of a Eurofer steel box, reinforced by an internal grid of radial-poloidal and poloidal-toroidal plates in order to withstand water pressure (155 [bar]) in case of accidental pressurization. In the module there are 15 stiffening plates in toroidal direction and 5 stiffening plates in poloidal direction. The module box results divided into 16 breeder units (BUs), whose dimensions are 824x234x147 [mm<sup>3</sup>], in poloidal direction and 6 channels in toroidal direction. Divided in the middle by a baffle plate, in each breeder unit the Pb-15.7Li enters from the bottom, flows in radial-poloidal direction and exits from the top.

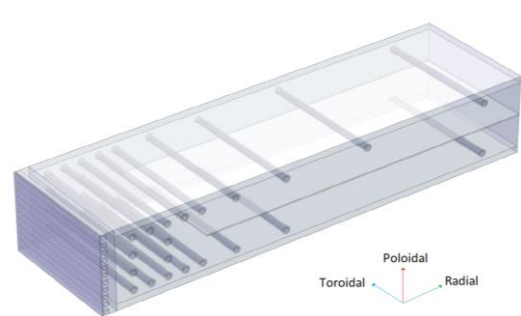


Fig. 1 – Representation of a WCLL breeder unit of the outboard equatorial module.

### 2.1 Governing Equations and Solution Technique

Under the Boussinesq hypothesis, which assumes that the density variation  $\Delta\rho$  has no effect on the flow field, except the one that gives rise to a buoyancy force, the incompressible formulation of the Navier-Stokes equations assumes the form:

$$\nabla \cdot \vec{u} = 0 \quad (1)$$

$$\rho_0(\vec{u} \cdot \nabla \vec{u}) = -\nabla p + \mu \nabla^2 \vec{u} + (\rho_0 + \Delta \rho) \vec{g} \quad (2)$$

where  $\rho_0$  [kg m<sup>-3</sup>] is the density evaluated at the average temperature of the Pb-15.7Li,  $\vec{u}$  [m s<sup>-1</sup>] is the velocity vector,  $p$  is the pressure field [Pa], and  $\mu$  [Pa s] is the dynamic viscosity. It must be observed that the velocity field of the Pb-15.7Li has been described using the k-epsilon turbulent model. Eqs. (1-2) are simultaneously solved with the convective-conductive heat transfer equation:

$$\rho_i c_{p,i} \vec{u} \cdot \nabla T_i + \nabla \cdot (-k_i \nabla T_i) = \dot{Q}_i \quad (3)$$

where  $T_i$  [K] is the temperature in the  $i$ -th domain (lead-lithium, Eurofer, coolant),  $c_{p,i}$  [J kg<sup>-1</sup> K<sup>-1</sup>] is the specific heat at constant pressure,  $k_i$  [W m<sup>-1</sup> K<sup>-1</sup>] is the thermal conductivity and  $\dot{Q}_i$  [W m<sup>-3</sup>] is the volumetric heat generation rate. The steady-state solution of temperature, pressure, and velocity has been used as an input for the general tritium transport equation:

$$\frac{\partial c_i}{\partial t} + (\nabla \cdot \vec{u}) c_i + \nabla \cdot (-D \nabla c_i) = s_i \quad (4)$$

where  $c_i$  is the tritium concentration,  $D_i$  [m<sup>2</sup> s<sup>-1</sup>] is the diffusion coefficient of tritium and  $s_i$  [mol m<sup>-3</sup> s<sup>-1</sup>] is the molar tritium generation rate along the radial coordinate. It must be noticed that both the volumetric heat generation rate and the molar tritium generation rate are space-dependent along the radial coordinate [7]. The materials properties have been taken from [8].

## 2.2 Summary of the main boundary conditions

The continuity of the pressure at Pb-15.7Li/Eurofer interface can be expressed introducing the partition coefficient  $K_j$  i.e. the ratio between the Sieverts' constant of tritium in Eurofer and the Sieverts' constant of tritium in the liquid metal:

$$c_2 = \frac{k_{s,Eu}}{k_{s,LM}} \cdot c_1 = K_j \cdot c_1 \quad (5)$$

where  $c_1$  [mol m<sup>-3</sup>] is the tritium concentration in lead-lithium and  $c_2$  [mol m<sup>-3</sup>] is the tritium concentration in Eurofer,  $j$  refers to horizontal stiffening plates (hSP), baffle or pipes. The flux continuity at Eurofer/water interface has also to be guaranteed:

$$(-D_{T_2,w} \nabla c_3 + c_3 \cdot \vec{u}) \cdot \hat{n}|_{w/Eu} = -k_d \cdot p_{T_2,w} + k_r \cdot c_2^2 \quad (6)$$

$$(-D_{T,Eu} \nabla c_2) \cdot \hat{n}|_{Eu/w} = 2(k_d \cdot p_{T_2,w} - k_r \cdot c_2^2) \quad (7)$$

where  $D_{T_2,w}$  [m<sup>2</sup> s<sup>-1</sup>] and  $D_{T,Eu}$  [m<sup>2</sup> s<sup>-1</sup>] are the diffusion coefficient of tritium in water and Eurofer, respectively,  $\hat{n}$  is the normal vector,  $c_3$  [mol m<sup>-3</sup>] is the tritium concentration in the water domain,  $k_d$  [mol s<sup>-1</sup> m<sup>-2</sup> Pa<sup>-1</sup>] is the dissociation coefficient, and  $k_r$  [m<sup>4</sup> mol<sup>-1</sup> s<sup>-1</sup>] is the recombination coefficient and  $p_{T_2,w}$  [Pa] is the tritium partial pressure in the water, related to Henry's law of solubility [9-10]. The inlet boundary condition at each domain has been set equal to zero, whereas at the outlet it

has been supposed that the diffusion contribution is much smaller than the convective contribution:

$$c_i = c_{0,i} \quad (8)$$

$$(-D_i \nabla c_i + c_i \cdot \vec{u}) \cdot \hat{n} = c_i \cdot \vec{u} \cdot \hat{n} \quad (9)$$

Eq. (8) is equivalent to assume that the extraction out of the blanket is perfect [9]. Initial conditions have been set to zero. The main input data used for the calculations are reported in Table 1.

Table 1 – Main input data for the WCLL breeder unit.

Parameter	Value	Description
$T_{in,LM}$	325 [°C]	Pb-15.7Li inlet temperature
$p_{LM}$	5 [bar]	Pb-15.7Li inlet pressure
$v_{LM}$	1 [mm s <sup>-1</sup> ]	Pb-15.7Li inlet velocity
$\Phi_{sup}$	0.5 [MW m <sup>-2</sup> ]	Heat flux on the first wall
$T_{in,w}$	285 [°C]	Water pipes inlet temperature
$v_{w,FW}$	1.24 [m s <sup>-1</sup> ]	Water pipes inlet velocity in the first wall
$v_{w,BZ}$	1.57 [m s <sup>-1</sup> ]	Water pipes inlet velocity in the breeder zone
$p_w$	155 [bar]	Water inlet pressure

## 2.3 Inventories and losses

Tritium inventories in the different domains have been estimated by means of the triple integral:

$$I_{WCLL,i}(t) = M_T \cdot \iiint c_i(\vec{x}, t) \cdot dV_i \quad (10)$$

where  $I_{WCLL,i}$  [g] is the tritium inventory for the WCLL BU in the  $i$ -th domain (Pb-15.7Li, Eurofer and water),  $M_T$  [g mol<sup>-1</sup>] is the atomic/molecular weight of tritium,  $c_i$  [mol m<sup>-3</sup>] is the concentration and  $V_i$  [m<sup>3</sup>] is the volume of the  $i$ -th domain. According to [11], tritium losses have been defined as the ratio of the tritium permeated through the Eurofer pipes, baffle and hSPs to the total tritium generated inside the lead-lithium eutectic:

$$\Phi_{WCLL}(t) = 100 \cdot \frac{\iint J_{perm}(\vec{x}, t) \cdot dA_i}{\iiint s(\vec{x}, t) \cdot dV_{LM}} \quad (11)$$

where  $\Phi_{WCLL}$  [%] is the tritium losses in WCLL BU and  $J_{perm}$  [mol m<sup>-2</sup> s<sup>-1</sup>] is the total flux that permeates from the Pb-15.7Li domain into the Eurofer domain.

## 3. Results

In this section, the main results concerning the effect of buoyancy on velocity fields, temperature fields, and, in particular, on the tritium transport are shown. The comparison with the results of the case without buoyancies is performed assuming the ones reported in [9].

### 3.1 Thermo-fluid-dynamics calculation

The temperature profile and the velocity field of Pb-15.7Li are shown in Fig. 2 and Fig. 3, for a radial poloidal cut plane passing from the middle of the breeder unit. The maximum temperature, 354 °C, shows a 27.8% decrease with respect to the no buoyancy case, whereas the average temperature is decreased by 12%. The buoyancy force tends to smooth the temperature field.

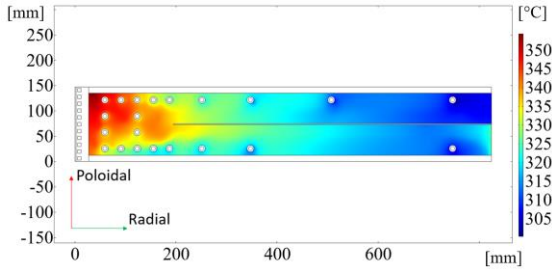


Fig. 2 – Temperature field [°C] in presence of buoyancy force.

The velocity field is reported in Fig. 3. The field of motion is affected by the density variation, where it is possible to observe the formation of recirculation patterns below and above the baffle.

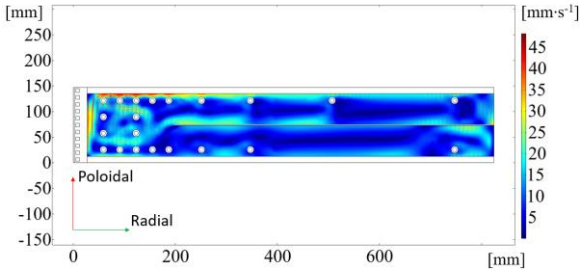


Fig. 3 – Velocity field [mm s<sup>-1</sup>] in presence of buoyancy force.

The highest velocities are localised at the interface with the upper horizontal stiffening plate, with a maximum value equal to 46.6 [mm s<sup>-1</sup>], whereas the maximum value without buoyancies was found to be 3.5 [mm s<sup>-1</sup>].

### 3.2 Tritium transport

Tritium transport calculations have been carried out considering an exponential decreasing tritium generation rate varying along the radial coordinate but constant in time, i.e. assuming DEMO to be operated at steady-state conditions [9,11]. The concentration distribution at  $t = 3$  [h] in the lead-lithium domain for a radial poloidal cut plane passing from the middle of the breeder unit is reported in Fig. 4.

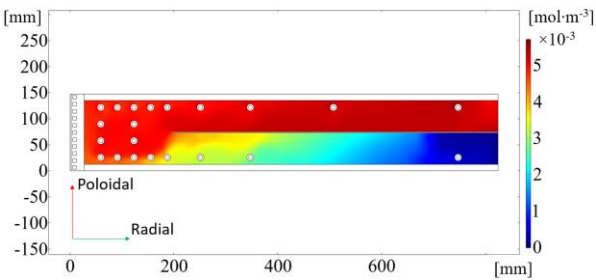


Fig. 4 – T concentration distribution [mol m<sup>-3</sup>] in the Pb-15.7Li domain.

It can be noticed that the tritium concentration above the baffle reaches the highest values with respect to the rest of the breeder unit ( $5.66 \cdot 10^{-3}$  [mol m<sup>-3</sup>]). In particular, the concentration increases when departing from the Pb-15.7Li entrance and decreases when moving from the first wall to the BU exit. Moreover, the time needed to reach the steady-state condition has been compared with the case without buoyancy forces [9], and it resulted considerably decreased, passing from 1200 to 35 minutes. This is due to the advection, which acts a significant role, due to the buoyancy effect.

Concerning the Eurofer domain, the tritium concentration in the horizontal stiffening plates and in the baffle are almost the same, whereas it is 22% higher in the Eurofer pipes. The average tritium concentration in Pb-15.7Li and Eurofer domains is shown in Fig. 5.

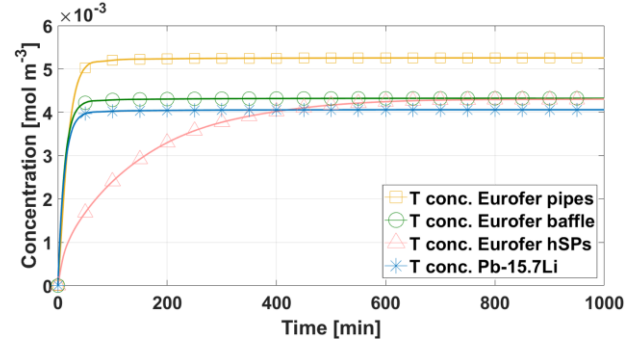


Fig. 5 – Average T concentration [mol m<sup>-3</sup>] in Pb-15.7Li and Eurofer domain.

Once tritium from monoatomic form recombines in diatomic form, it interacts with the naturally solved hydrogen present in water according to the reactions:



For this analysis, it has been assumed that chemical equilibrium instantaneously occurs; for both Equations (12) and (13); the chemical equilibrium constants have been derived from [12] and [13], respectively. The profile of the recombined tritium has been used as an input for the chemical calculation, performing an a posteriori evaluation in order to simplify the treatment of the isotopic exchange rate. In Fig. 6, the average tritium concentration is shown for column 1, 3, 5, 7 and 9, where a column is defined as the set of poloidal tubes that are encountered moving from the FW to the Pb-15.7Li exit.

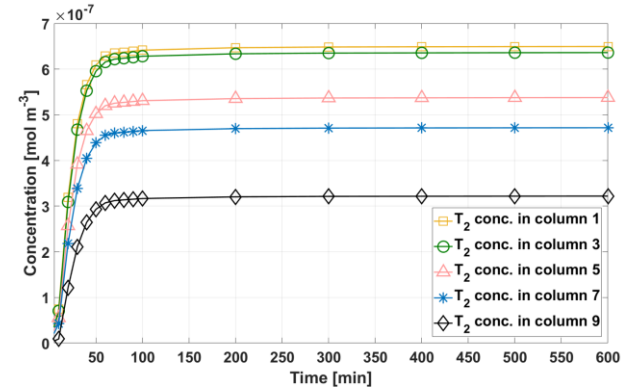


Fig. 6 – Average T<sub>2</sub> concentration [mol m<sup>-3</sup>] in the water domain.

The concentration is decreasing when moving from the first wall to the Pb-15.7Li exit. The time needed to reach the steady-state condition is reduced of about one order of magnitude lower with respect to the case without buoyancy [9]. The time to reach 95% of asymptotic concentration for each domain is reported in Table 2, for the case without buoyancy (NB) and with buoyancy (B) effect. The concentration in water has been referred to as HTO form, since all T<sub>2</sub> reacts with hydrogen and HT concentration is small when compared to HTO.

Table 2 – Concentrations and times to reach asymptotic condition for the buoyancy case in WCLL breeder unit.

	$c_{eq,B}$ [mol m <sup>-3</sup> ]	$c_{eq,NB}$ [mol m <sup>-3</sup> ]	$t_B^*$ [min]	$t_{NB}^*$ [min]
T in Pb-15.7Li	$4.03 \cdot 10^{-3}$	$3.29 \cdot 10^{-3}$	35	1200
T in Eurofer (pipes)	$5.24 \cdot 10^{-3}$	$1.09 \cdot 10^{-2}$	45	1300
T in Eurofer (baffle)	$4.34 \cdot 10^{-3}$	$1.79 \cdot 10^{-3}$	37	200
T in Eurofer (hSPs)	$4.29 \cdot 10^{-3}$	$7.30 \cdot 10^{-3}$	520	2000
HTO in Water	$1.11 \cdot 10^{-6}$	$2.52 \cdot 10^{-6}$	51	1100

The tritium partial pressure has been derived from Sieverts' law using Reiter's correlation [14], and it has found to be on average 21 [Pa].

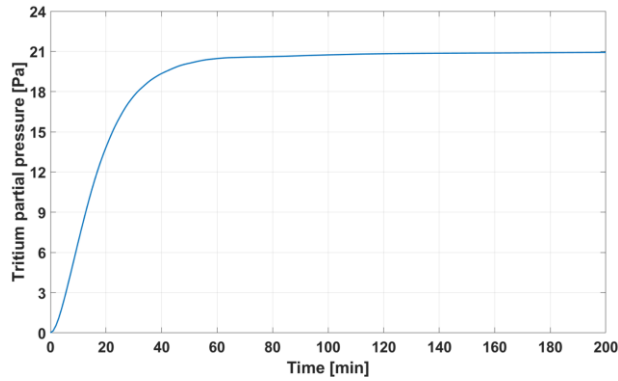


Fig. 7 – Average T partial pressure [Pa] in the Pb-15.7Li domain.

Tritium inventories and losses are evaluated by means of Eqs. (10-11) and reported in Table 3.

Table 3 – Asymptotic T inventories and losses for the buoyancy case and no buoyancy case in WCLL breeder unit.

	Inventories	
	Buoyancy	No Buoy. [7]
Inv. in Pb-15.7Li [μg]	266.7	219.0
Inv. in Eurofer (pipes) [μg]	7.1	14.8
Inv. in Eurofer (baffle) [μg]	3.9	1.6
Inv. in Eurofer (hSPs) [μg]	58.0	99.7
Inv. in Eurofer (total) [μg]	69.0	116.1
Inv. in Water [μg]	$5.42 \cdot 10^{-3}$	$1.29 \cdot 10^{-2}$
Total [μg]	335.7	335.1
	Losses	
Total [%]	13.3	11.0

In the case of buoyancy, the tritium retention in Pb-15.7Li constitutes the 79.4% of the total inventory, whereas in [9] it constitutes the 65.4%; the buoyancy force tends to increase the inventory in the liquid metal, decreasing the permeated flux towards the steel. It can be noticed that the overall tritium mass balance is conserved. Concerning tritium losses, they are almost equal both for buoyancy and no buoyancy case.

#### 4. Conclusions

A tritium transport study has been performed for a generic breeder unit belonging to the outboard equatorial module of the WCLL breeding blanket. A multiphysics approach has been adopted, including interface phenomena, tritium generation rate profile, thermal fields and velocity field of the lead-lithium; the buoyancy forces have been implemented starting from a reference case [9].

The fluid motion and the temperature field are strongly modified under the action of buoyancies; in particular, the velocity field presents a formation of vortexes which create different patterns of circulation and locally increases the maximum velocity up to 46.6 [mm s<sup>-1</sup>], whereas the temperature field appears to be smoothed out, with a decrease of maximum and average temperatures of 27.8% and 12%. The modification of velocity and temperature field has an impact on the tritium transport; the long response time of the reference case [9], where diffusion is dominant with respect to advection, is deeply reduced due to the presence of vortexes, which increase the advection contribution. This causes in one side higher tritium retention in the liquid metal (79.4%), on the other one lower retention in the steels, values which are higher with respect to the reference case. Hence, the inventory on the water results to be about one half the inventory of the case without buoyancies. The average value of tritium partial pressure in the lead-lithium has been found to be 21 [Pa].

Future work will regard the implementation of the magneto-hydro-dynamics effect in order to investigate the direct effect on the velocity field and as consequences the impact on the tritium concentrations, inventories and losses.

#### References

- [1] Federici G, et al. DEMO design activity in Europe: Progress and updates. *Fus Eng Des* 2018; 136 (Pt A): 729-41.
- [2] Turnyanskiy M, et al. European roadmap to the realization of fusion energy: mission for solution on heat-exhaust systems. *Fus Eng Des* 2015; 96-97: 361-4.
- [3] Maisonnier D, et al. DEMO and fusion power plant conceptual studies in Europe. *Fus Eng Des* 2006; 81 (8-14): 1123-30.
- [4] Fischer U., et al. Neutronics requirements for a DEMO fusion power plant. *Fus Eng Des* 2015; 98-99: 2134-37.
- [5] Candido L, et al. Tritium transport in HCLL and WCLL DEMO blankets. *Fus Eng Des* 2016; 109-111 (Pt A): 248-54.
- [6] COMSOL Multiphysics. Version 5.3a. Available on-line: <http://www.comsol.com/>
- [7] Del Nevo A, et al. Integration for WCLL in 2015/DDD 2015 for WCLL (update of DDD 2014). Final Report on Deliverable. Camugnano (BO): ENEA C. R. Brasimone, Department for Fusion and Nuclear Safety Technologies; 2016. Report no. BB-3.1.2-T004-D001.
- [8] Martelli D, et al. Literature review of lead-lithium thermophysical properties. *Fus Eng Des* 2019; 138: 183-95.
- [9] Candido L, et al. Tritium transport model at the minimal functional unit level for HCLL and WCLL breeding blankets of DEMO. *Fus Eng Des* 2018; 136 (Pt B): 1327-31.
- [10] Harvey AH. Semiempirical correlation for Henry's constants over large temperature ranges. *AIChE J* 1996; 42: 1491-94.
- [11] Zhang H, et al. Quantification of dominating factors in tritium permeation in Pb-15.7Li blankets. *Fus Sci Tech* 2015; 68 (2): 362-7.

- [12] Jones WM, Thermodynamic Functions for Tritium and Tritium Hydride. The Equilibrium of Tritium and Hydrogen with Tritium Hydride. The Dissociation of Tritium and Tritium Hydride, J Chem Phys 1948; 16 (11): 1077-81.
- [13] Black JF, and Taylor HS. Equilibrium in Hydrogen-Water Systems Containing Tritium. J Chem Phys 1943; 11 (9): 395-402.
- [14] Reiter F, Solubility and diffusivity of hydrogen isotopes in liquid Pb-17Li. Fus Eng Des 1991; 14 (3-4): 207-11.